Ordered and chaotic behavior of two coupled van der Pol oscillators

I. Pastor
Asociación EURATOM/CIEMAT para Fusión, Avenida Complutense 22, 28040 Madrid, Spain

Víctor M. Pérez-García
Departamento de Física Teórica I, Facultad de Ciencias Físicas, Universidad Complutense, Ciudad Universitaria s/n, E-28040 Madrid, Spain

F. Encinas-Sanz* and J. M. Guerra*
Departamento de Optica, Facultad de Ciencias Físicas, Universidad Complutense, Ciudad Universitaria s/n, E-28040 Madrid, Spain
(Received 16 March 1992; revised manuscript received 28 December 1992)

A physically intuitive, highly symmetric coupling of two van der Pol oscillators is considered here. The structure of the equilibrium points and the discrete symmetries of the model equations are discussed. For some combinations of the parameters, infinitely many equilibrium points appear and evidence is presented pointing to the existence of infinite periodic trajectories. A complete characterization of the dynamics is done on three specific cases, as a function of the coupling parameters. It is found that several attractors coexist in phase space, either having the symmetry of the model equations or appearing in pairs that restore such symmetry. The possibility that the asymptotic dynamics is different in the coexisting symmetric and asymmetric attractors is investigated, along with their creation or destruction, splitting, and merging, when a control parameter is varied. The presence of several attractors allows the points in phase space to change from one basin to another when a control parameter is changed. The route to chaos is through period doubling when only one attractor is explored. When oscillators lock onto an ordered behavior, the period and amplitude surfaces are computed as a function of the (two) coupling parameters and compared with those periods and amplitudes for the corresponding unperturbed oscillators.

PACS number(s): 05.45.+b, 42.65.Vh

I. INTRODUCTION

It has already been fairly well established that the dynamics of very simple physical systems can be quite complex, if a sufficient amount of nonlinearity is present. From the mathematical point of view, the nonlinear (ordinary) differential equations governing such systems are not amenable to a closed-form solution, but instead present a variety of behaviors that are far from trivial and not totally mastered at present. Geometric and numerical methods have allowed us, nevertheless, to gain a good general picture of the situation, with terms such as bifurcations, strange attractors, Lyapunov exponents, and metric entropy being commonplace. In addition, the scope and range of physical systems displaying "deterministic chaos" has grown considerably and examples can be found in optics [1], laser physics [2], fluid mechanics [3, 4], chemical reactions [5], plasma physics [6], electronics [7], etc.

In electronics, nonlinear oscillators have been used for a long time as very efficient and powerful systems for obtaining frequency conversion, multiplication, demultiplication, and generation of higher harmonics from a given signal [8]. That makes the coupling of nonlinear oscillators a natural question from the point of view of modern nonlinear dynamics theory.

In literature, the case of one nonlinear oscillator perturbed by a sinusoidal forcing [9–11] is highly documented; the dynamics found at this stage can vary from locking to the external forcing frequency to apparently irregular (though deterministic) oscillations with a low correlation time and wide spectrum. Recently, the case of two coupled nonlinear oscillators has also been studied from dynamical systems theory point of view [12, 13]. In this paper we focus on the coupling of two van der Pol oscillators studying the dynamics as a function of the (two) coupling parameters using Fourier analysis, bifurcation diagrams, time histories, phase space portraits, and the Grassberger-Procaccia (GP) algorithm as tools for the investigation. We believe that this research complements the above-mentioned case of a forced nonlinear oscillator, illustrating the order and chaos in a system not subject to any external driving, but to the self-sustaining dynamics of its components.

Let us write down the normalized adimensional equation describing the van der Pol oscillator [8]

$$\frac{d^2x}{dt^2} - (\epsilon - x^2)\frac{dx}{dt} + x = 0 \tag{1}$$

or, introducing the new function $y = \frac{dx}{dt}$,

$$\frac{dx}{dt} = y, \quad \frac{dy}{dt} = (\epsilon - x^2)y - x. \tag{2}$$

Equations (2) contain only one parameter, which determines essentially the size and shape of the unique stable limit cycle described by them. For $\epsilon \ll 1$, (2) describes nearly sinusoidal oscillations, while for $\epsilon \gg 1$ relaxation oscillations are found.

The model equations we are going to study are the following:

$$\begin{aligned} \frac{dx}{dt} &= y, \\ \frac{dy}{dt} &= [\epsilon_1 - (x+\beta z)^2]y - (x+\beta z), \\ \frac{dz}{dt} &= v, \\ \frac{dv}{dt} &= [\epsilon_2 - (z+\alpha x)^2]v - (z+\alpha x). \end{aligned} \tag{3}$$

As is evident, for $\alpha = \beta = 0$, Eqs. (3) describe two uncoupled van der Pol oscillators, with their limit cycles (and hence their amplitudes and periods) governed by the values of ϵ_1, ϵ_2. The coupling considered can be easily interpreted as a "perturbation" of each oscillators' amplitude through a signal proportional to the amplitude of the other.

From an experimental point of view the simulation of Eq. (3) with an electronic analogical computer is straightforward. Originally, the van der Pol oscillator was a vacuum tube oscillator [8] and the proposed coupling of two such oscillators could be performed easily. The coupling between two laser oscillators is another experimental system related to the model considered here because of the well-known fact that the laser field (in the rotating-wave approximation) obeys a differential equation with a van der Pol type nonlinearity [14, 15].

We have studied three cases consisting of values for $\epsilon_1, \epsilon_2 = 0.1, 1.0; 1.0, 1.0$; and $1.0, 2.0$. The selection of the three specific pairs of values for ϵ_1, ϵ_2 is motivated by our desire to study the coupling in three regimes: one oscillator is almost sinusoidal and the other moderately nonlinear ($\epsilon_1 = 0.1, \epsilon_2 = 1.0$); two exactly equal moderately nonlinear oscillators ($\epsilon_1 = 1.0, \epsilon_2 = 1.0$); and one moderately nonlinear oscillator and the other quite so ($\epsilon_1 = 1, 0, \epsilon_2 = 2.0$). For each case α and β have been varied in a systematic way, going from a weak coupling to values of about one.

The rest of the paper is organized as follows. In Sec. II the existence and structure of equilibrium points and of the discrete symmetries of model equations are discussed. Section III presents the numerical results obtained from the numerical integration of Eqs. (3), and Sec. IV summarizes the conclusions.

II. EQUILIBRIUM POINTS AND DISCRETE SYMMETRIES OF MODEL EQUATIONS

System (3) may be expressed as

$$\frac{d\mathbf{r}}{dt} = \underline{A}\mathbf{r} + \mathbf{N}(\mathbf{r}), \tag{4}$$

where

$$\mathbf{r} = \begin{pmatrix} x \\ y \\ z \\ v \end{pmatrix}, \tag{5}$$

$$\underline{A} = \begin{pmatrix} 0 & 1 & 0 & 0 \\ -1 & \epsilon_1 & -\beta & 0 \\ 0 & 0 & 0 & 1 \\ -\alpha & 0 & -1 & \epsilon_2 \end{pmatrix}, \tag{6}$$

$$\mathbf{N}(\mathbf{r}) = \begin{pmatrix} 0 \\ f(\mathbf{r}) \\ 0 \\ g(\mathbf{r}) \end{pmatrix}, \tag{7}$$

and

$$f(\mathbf{r}) = -(x+\beta z)^2 y, \quad g(\mathbf{r}) = -(z+\alpha x)^2 v. \tag{8}$$

Equilibrium points for Eqs. (3) are obtained by equating the right-hand side to zero. Thus

$$y = 0, \quad x + \beta z = 0, \quad v = 0, \quad z + \alpha x = 0. \tag{9}$$

Combining the equations in (9) we obtain $(1-\alpha\beta)x = 0$ and $(1-\alpha\beta)z = 0$. Thus, except for the case $\alpha\beta = 1$, the origin $x = y = z = v = 0$ is the only equilibrium point.

The determinant of the matrix $\underline{A}$ is equal to $1-\alpha\beta$. On the other hand, $f(\mathbf{r})$ and $g(\mathbf{r})$ and their partial derivatives are regular and satisfy

$$\lim_{|\mathbf{r}|\to\infty} \frac{f(\mathbf{r})}{|\mathbf{r}|} = 0, \quad \lim_{|\mathbf{r}|\to\infty} \frac{g(\mathbf{r})}{|\mathbf{r}|} = 0. \tag{10}$$

Consequently, the equilibrium point

$$\mathbf{r}_e = \begin{pmatrix} 0 \\ 0 \\ 0 \\ 0 \end{pmatrix} \tag{11}$$

is isolated and simple when $\alpha\beta \neq 1$ [16].

By linearizing (4) around the critical point (11) we obtain

$$\frac{d\mathbf{r}}{dt} = \underline{A}\mathbf{r}. \tag{12}$$

From (12), the characteristic polynomial

$$|\underline{A} - \lambda \underline{I}| = 0 \tag{13}$$

is explicitly expressed as

$$\lambda^4 - (\epsilon_1+\epsilon_2)\lambda^3 + (2+\epsilon_1\epsilon_2)\lambda^2 - (\epsilon_1+\epsilon_2)\lambda + (1-\alpha\beta) = 0. \tag{14}$$

Because of the highly symmetric coupling considered here, the eigenvalues given by (14) depend only on three parameters $(\epsilon_1+\epsilon_2, \epsilon_1\epsilon_2, \alpha\beta)$ and are invariant under the transformations $\epsilon_1 \leftrightarrow \epsilon_2, \alpha \leftrightarrow \beta$.

The eigenvalues of (14) have been computed for the pairs of values $\epsilon_1, \epsilon_2 = (0.1, 1.0), (1.0, 1.0)$, and $(1.0, 2.0)$ as a function of the parameter $\Delta = 1 - \alpha\beta$, Δ varying

between -20.0 and 20.0. The evolution of the eigenvalues on the complex plane is shown in Fig. 1.

It can be seen that Eq. (14) generally has two purely real and two complex conjugate roots, all of them with a real part different from zero. Thus the critical point (11) is a hyperbolic one, except for some isolated values of the parameter Δ.

If $\alpha\beta = 1$, then the manifold of equilibrium points is found to be a line in $\mathbb{R}^4$, namely $y = v = 0, x = -\beta z$. It seems appropriate to point out the fact that for this special combination of coupling parameters, *infinitely many* new equilibrium points appear, and that is a nonstandard feature of the model equations studied.

We have also obtained the linearized equations around an arbitrary equilibrium point of the form $x_e = \gamma, y_e = 0, z_e = -\alpha\gamma, v_e = 0$ when $\alpha\beta = 1$. Introducing new variables $x' = x - x_e, y' = y - y_e, z' = z - z_e$, and $v' = v - v_e$,

$$\frac{d\mathbf{r}'}{dt} = \underline{A}\mathbf{r}'. \tag{15}$$

From (15), the characteristic polynomial is found to be

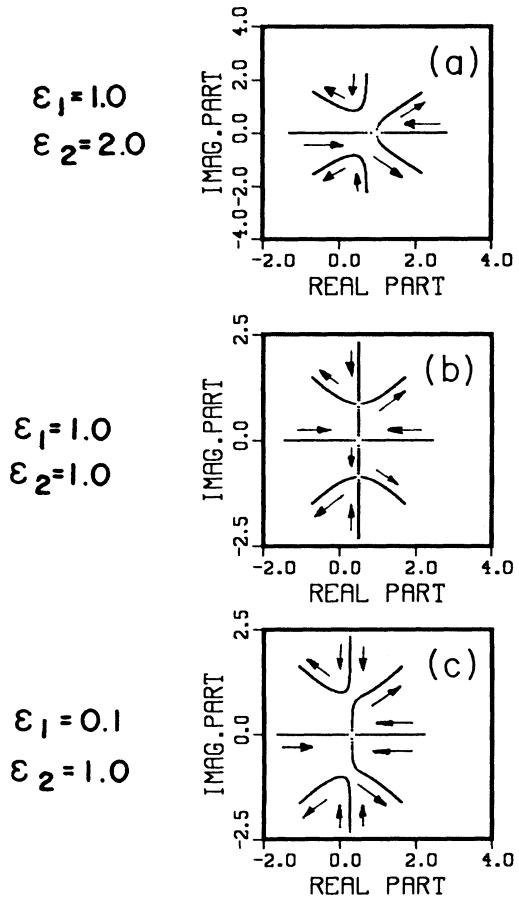

FIG. 1. Curves generated by the motion of the eigenvalues of (14) in the complex plane as a function of the parameter Δ varying in the range $\Delta \in [-20.0, 20.0]$. The other parameters have values (a) $(\epsilon_1, \epsilon_2) = (0.1, 1.0)$, (b) $(\epsilon_1, \epsilon_2) = (1.0, 1.0)$, and (c) $(\epsilon_1, \epsilon_2) = (1.0, 2.0)$.

$$\lambda[\lambda^3 - (\epsilon_1 + \epsilon_2)\lambda^2 + (2 + \epsilon_1\epsilon_2)\lambda - (\epsilon_1 + \epsilon_2)] = 0. \tag{16}$$

Thus

$$\lambda^3 - (\epsilon_1 + \epsilon_2)\lambda^2 + (2 + \epsilon_1\epsilon_2)\lambda - (\epsilon_1 + \epsilon_2) = 0,$$

$$\lambda = 0. \tag{17}$$

Some conclusions can be drawn from (17), the most important being that the type of linear equilibrium is independent of the point considered in the manifold of equilibrium points [(17) is independent of α]. In addition, $\lambda = 0$ is always an eigenvalue corresponding to the normalized eigenvector $(1, 0, -\alpha, 0)/\sqrt{(1 + \alpha^2)}$, which spans the linear space of the equilibrium points. Eigenvalues depend only on two independent parameters $(\epsilon_1 + \epsilon_2, \epsilon_1\epsilon_2)$ and are invariable through changes $\epsilon_1 \leftrightarrow \epsilon_2$.

Equations (3) admit some symmetries that are found to be relevant for the analysis and interpretation of the dynamics. All of them can be easily verified.

Proposition 1. Let $x(t), y(t), z(t), v(t)$ be a solution of (3) for parameters $\epsilon_1, \epsilon_2, \alpha, \beta$; then $-x(t), -y(t), -z(t), -v(t)$ is also a solution for the same set of parameters.

Proposition 2. Let $x(t), y(t), z(t), v(t)$ be a solution of (3) for parameters $\epsilon_1, \epsilon_2, \alpha, \beta$; then $x(t), y(t), -z(t), -v(t)$ is also a solution for parameters $\epsilon_1, \epsilon_2, -\alpha, -\beta$.

Proposition 3. Let $x(t), y(t), z(t), v(t)$ be a solution of (3) for parameters $\epsilon_1, \epsilon_2, \alpha, \beta$; then $-z(t), -v(t), x(t), y(t)$ is also a solution making the new identification of parameters $\alpha \leftrightarrow -\beta, \beta \leftrightarrow -\alpha, \epsilon_1 \leftrightarrow \epsilon_2$.

Of special interest for our purposes are propositions 1 and 2. Proposition 1 implies that attractors in phase space have to be symmetric by inversion with respect to the origin, or, if this is not the case, they must appear in pairs, to restore the exact symmetry of model equations. Besides making the existence of several attractors in phase space plausible (confirmed numerically by the results in Sec. III), this exact symmetry is a very good way to test the scheme used for numerical integration, since the attractors calculated numerically must have the symmetry of the underlying equations or appear in (symmetric) pairs.

We have also made use of proposition 2, when computing the dynamics as a function of parameters α, β. In fact, proposition 2 implies that it is enough to study the dynamics for arbitrary $\alpha \geq 0, \beta$ to know the behavior on the whole $\alpha\beta$ plane. The dynamics for α, β is just the same as the one for $-\alpha, -\beta$ except for a trivial, specular reflection around the x axis (if we look at the x-z projection of phase space). Proposition 3 implies that for the special case $\epsilon_1 = \epsilon_2$, the dynamics on the $\alpha\beta$ plane is invariable under reflection around the line $\beta = -\alpha$. As pointed out before, propositions 1–3 have been used to check the numerical integration scheme used.

III. NUMERICAL RESULTS

A standard Runge-Kutta algorithm with automatic step size control and double precision (NAG library routine D02BAF) has been used to integrate numerically

model equations (3). To improve the efficiency in computation time, (3) are integrated with two different initial time steps, one allowing a low-precision fast computing of the transient behavior, and the other allowing a high-precision integration, once the steady state has been reached. Equations (3) have been integrated from $t = 0$ to $t = 1000$, with a time step equal to 0.1 in order to make transients disappear, and then with a step size equal to 0.01 or 0.005.

The techniques used to diagnose the dynamics have been phase-space projections of the attractor(s) on the x-z plane, time histories for variables x and z, bifurcation diagrams for both variables, Fourier analysis, and the GP algorithm. The combined application of these techniques has allowed a quite complete characterization of the behavior of the two coupled oscillators.

A. Overview of the dynamical features of model equations

In Fig. 2 the main dynamical features of Eq. (3) are summarized, which qualitatively provides the kind of behavior arising for several points on the α-β plane (coupling parameters) for the three combinations of ϵ_1, ϵ_2 considered. Making use of proposition 2, the dynamics have been computed for $\alpha \geq 0$, β being either positive or negative, and the whole plot is obtained by inversion through the origin. In some particular cases, however, as stated in Sec. II, this point has been tested numerically to be sure that the integration scheme is working properly.

The information gathered in Fig. 2 has been obtained through visualization of the time histories of variables x and z and its projection on the x-z plane.

Some conclusions are apparent at this stage of the investigation: for $\alpha\beta > 0$, no trace of chaos has been found for the three cases studied; instead, the locking of the two oscillators occurs (limit cycle behavior). If $\alpha\beta > 1$ in cases $\epsilon_1 = 0.1, \epsilon_2 = 1.0, \epsilon_1 = \epsilon_2 = 1.0$, we obtain seemingly unbounded solutions [see Figs. 2(a) and 2(b)]. We have computed such solutions using a decreasing integration step size to discard the possibility of the integration not working well. Perhaps the main feature concerning such solutions is that asymptotically, one of the variables is monotonically increasing (decreasing), while the other is decreasing (increasing), but with a regular oscillation superimposed on it (Fig. 3). The variable that evolves monotonically when t goes to infinite can be either x or z. Since we are mainly interested in bounded oscillating behaviors, such solutions have not been investigated in much detail.

For $\alpha = 0$, β not being zero, or $\beta = 0$, α not being zero (one oscillator drives the other, but is not influenced by the second), we have obtained locking for cases $\epsilon_1 = 0.1, \epsilon_2 = 1.0$, and $\epsilon_1 = \epsilon_2 = 1.0$ and indications of chaos through period doubling in the case $\epsilon_1 = 1.0, \epsilon_2 = 2.0$.

If $\alpha\beta < 0$, the dynamics becomes richer in all the cases studied. It is apparent from Fig. 2 that when the two uncoupled oscillators become more nonlinear the area in the α-β plane occupied by the regular behavior decreases steadily, favoring chaotic solutions [Figs. 2(a)–2(c)].

Although both oscillators can be very different ($\epsilon_1 \gg \epsilon_2$ for instance) the coupling locks them to the same period, strongly dependent on the α and β coupling pa-

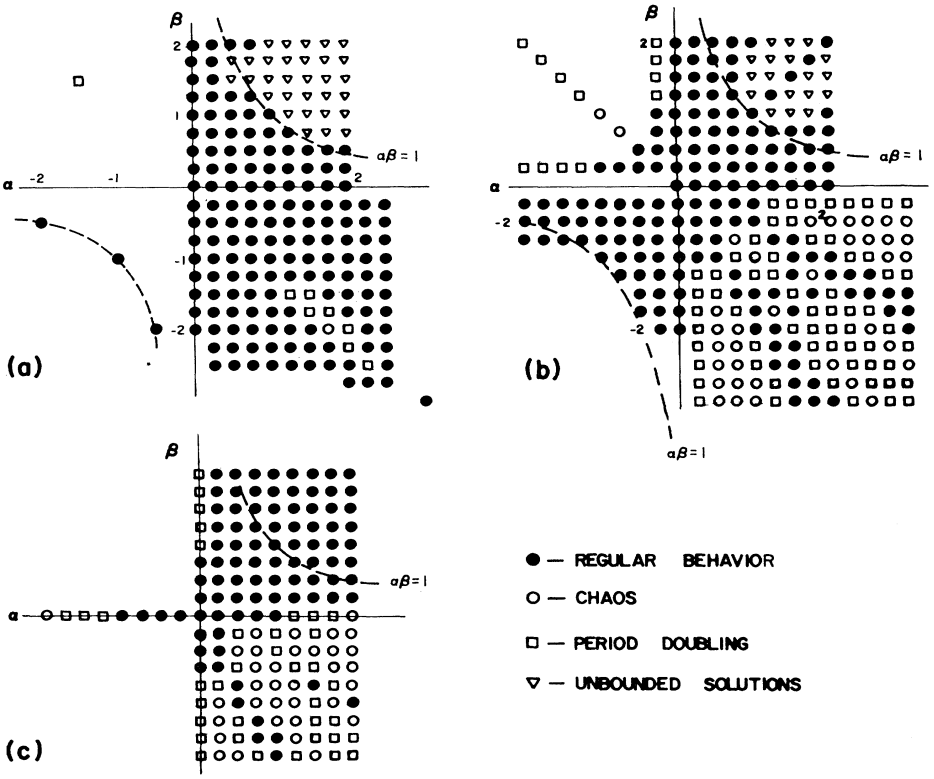

FIG. 2. Nature of the dynamics found by exploring a reticulum of points on the α and β planes. The other parameter values for the three cases analyzed correspond to (a) $(\epsilon_1, \epsilon_2) = (0.1, 1.0)$, (b) $(\epsilon_1, \epsilon_2) = (1.0, 1.0)$, and (c) $(\epsilon_1, \epsilon_2) = (1.0, 2.0)$.

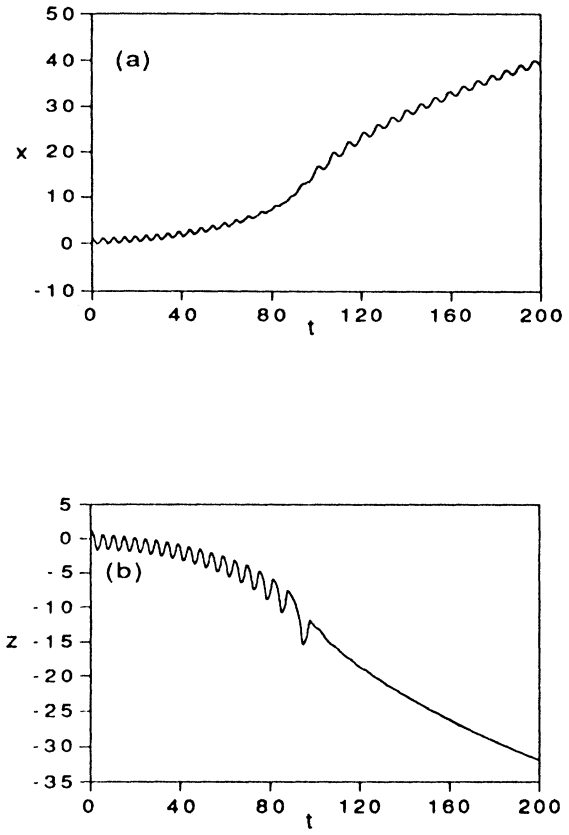

FIG. 3. Shape of the (a) $x(t)$ and (b) $y(t)$ functions with $\alpha\beta > 1$ and $\epsilon_1 = 0.1, \epsilon_2 = 1.0$.

rameters. Figure 4(a) shows the surface of the oscillation period $T(\alpha, \beta)$ in the case when $\epsilon_1 = 0.1, \epsilon_2 = 1.0$. The oscillation amplitude (defined as the difference between maximum and minimum) is very different in both oscillators and very dependent on α and β. This dependence $X(\alpha, \beta), Z(\alpha, \beta)$ also for the case where $\epsilon_1 = 0.1, \epsilon_2 = 1.0$ is plotted in Figs. 4(b) and 4(c).

B. Symmetry, attractors, and the transition order chaos

In this section we concentrate mainly on the $\alpha\beta < 0$ region of the coupling parameters' plane. Our goal will be to look closer at the dynamics, by computing bifurcation diagrams for some combinations of α and β, one parameter being fixed and the other varying in the range of interest. Furthermore, Fourier analysis for $x(t)$ and $z(t)$ will be performed and the GP algorithm will be used in certain particular cases. Table I summarizes the different combinations of parameters used for the computation of the bifurcation diagrams.

Figures 5 and 6 give relevant information about bifurcations. All bifurcation diagrams have been computed starting from the initial condition $x_0 = y_0 = z_0 = v_0 = 1.0$ and, after transients, by storing the values of the successive relative maxima for $x(t)$ and $z(t)$ as a function of the control parameter. In many of them the appearance of sudden jumps can be seen as the control parameter varies. This fact can be interpreted as follows: the initial point pertains to different basins for different values of α and β, this allowing for the jumps between the several

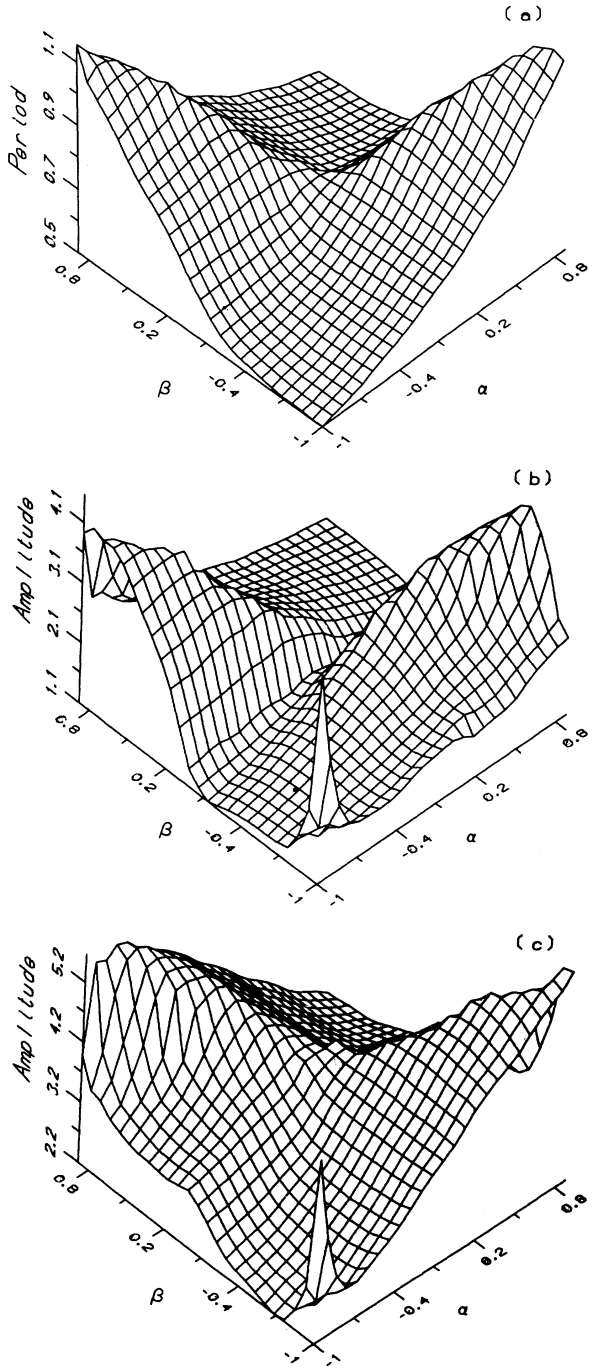

FIG. 4. (a) Surface of periods $T(\alpha, \beta)$, (b) surface of amplitudes for the first oscillator (X), and (c) surface of amplitudes for the second oscillator (Z), for parameter values $\epsilon_1 = 0.1, \epsilon_2 = 1.0$. The range of variation of the other parameters is $\alpha \in [0.89, -0.99], \beta \in [0.89, -0.99]$.

TABLE I. Parameter values for which a systematic study of the dynamics has been done. Last column is a reference for each concrete case in the text.

ϵ_1	ϵ_2	Fixed parameter	Variable parameter	Case
0.1	1.0	$\beta = -2.0$	$\alpha \in [1.5, 2.25]$	*b*1
0.1	1.0	$\alpha = 1.75$	$\beta \in [-2.25, -1.5]$	*b*2
1.0	1.0	$\beta = -1.75$	$\alpha \in [0.0, 1.0]$	*b*3
1.0	1.0	$\beta = -0.5$	$\alpha \in [1.0, 2.0]$	*b*4
1.0	1.0	$\beta = -3.0$	$\alpha \in [0.0, 1.5]$	*b*5
1.0	2.0	$\beta = -0.75$	$\alpha \in [0.0, 2.0]$	*b*6
1.0	2.0	$\beta = -2.0$	$\alpha \in [0.0, 1.0]$	*b*7
1.0	2.0	$\alpha = 1.0$	$\beta \in [-2.0, 0.0]$	*b*8

coexisting attractors in phase space. To further illustrate this point, we have chosen one bifurcation diagram (Table I, *b*5) and plotted the corresponding attractors for as many as 18 different values of the control parameter. Some results are given in Fig. 7. It can be seen how the initial point goes to attractors that change in location or form when the parameter is varied, and how some windows of order in the sea of chaotic behavior are present.

In some of the calculated bifurcation diagrams there is no evidence of more than one attractor (Table I, *b*4 and *b*7). In such cases the transition order chaos is more easily followed and found to occur through period doubling. We have illustrated this point for case *b*4 in Figs. 8–11 in which time histories, spectra, and attractors' projections are plotted.

A natural question arises concerning the number and dynamics of attractors in phase space as a function of a control parameter. Symmetry considerations alone are not enough to settle these questions concerning attractor creation, destruction, splitting, or merging.

Only two concrete examples have been attempted and not an exhaustive investigation. In the first case, the values $\epsilon_1 = 1.0$ and $\epsilon_2 = 2.0$ are chosen. We begin by taking $\beta = -0.75$ while the parameter α is finely varied from 0.970 to 1.100. For $\alpha = 0.970$ and evolving several initial conditions we only find one inversion symmetric strange

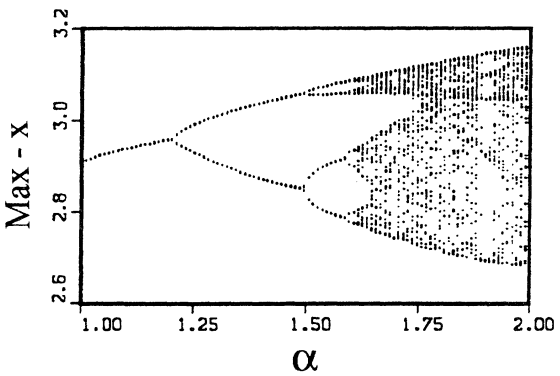

FIG. 5. Bifurcation diagram for x as a function of the parameter $\alpha \in [1.0, 2.0]$. The other parameters are fixed to $\epsilon_1 = 1.0, \epsilon_2 = 1.0, \beta = -0.5$.

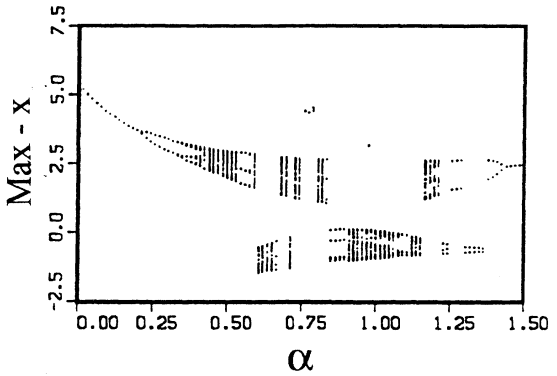

FIG. 6. Bifurcation diagram for x as a function of the parameter $\alpha \in [0.0, 1.5]$. The other parameters are fixed to $\epsilon_1 = 1.0, \epsilon_2 = 1.0, \beta = -3.0$.

attractor, but at $\alpha = 0.9805$ it splits into two strongly interwoven strange attractors (as projections on the x-z plane), one being the symmetric inversion of the other. For $\alpha = 1.000$, a small percentage of the evolved initial conditions bring us to two additional regular solutions (limit cycles). Meanwhile, the two strange attractors become progressively less interleaved (Fig. 12).

We have investigated the fractal dimension of attractors by means of the GP algorithm. The numerical computation was done by using a time series of 10 000 points covering about 30 periods of the x variable.

The application of the GP algorithm was done for α values around 0.9805, when the symmetric attractor splits into two nonsymmetric ones. For the symmetric attractor ($\alpha = 0.980$) a good slope convergence is found for a value $\nu = 1.4$; for $\alpha = 0.99$, when two nonsymmetric attractors coexist, a good slope convergence is found for the value $\nu = 1.6$.

Another interesting transition is observed for $\epsilon_1 = \epsilon_2 = 1.0, \beta = -1.75$ and α is varied between 0.480 and 0.500. For $\alpha = 0.480$, two strange attractors exist, one being symmetric by inversion of the other (Fig. 13). After a slight change in the value of α ($\alpha = 0.485$), two regular attractors (limit cycles) appear in 2% of the evolved initial conditions. A period doubling for the two limit cycles is observed at $\alpha = 0.4867$.

For $\alpha = 0.487$ the two limit cycles disappear, and one symmetric by inversion strange attractor is found, the two strange nonsymmetric isolated attractors that are symmetric by inversion of one another also remaining. A further increase in α enhances the size of the basin of the symmetric attractor.

Now the application of the GP test was done to the symmetric and asymmetric attractors coexisting for $\alpha = 0.5$. The slope converges for both attractors to the value $\nu = 1.6$ (Fig. 14).

As is well known Witney's [17] embedding theorem states that a separable C^r ($r \geq 1$) manifold of dimension ν can be faithfully embedded in a Euclidean space of dimension $2\nu + 1$. In our case the dimension of the phase space is the number of dependent variables in the set of first-order differential equations, which is 4. Then

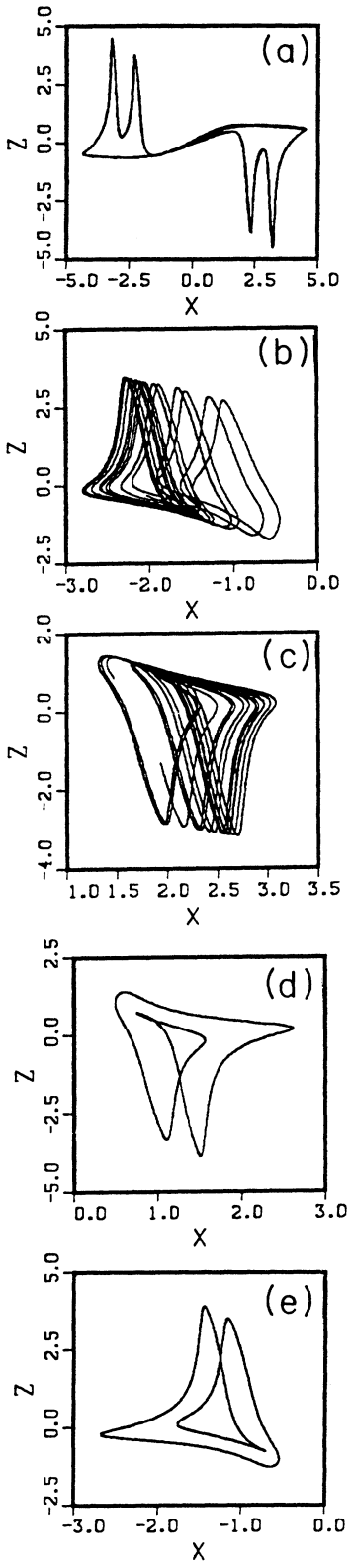

FIG. 7. Projections of the attractor on the x-z plane for eighteen α values in the range $[0.0, 1.0]$, the other parameters being fixed to $\beta = -3.0, \epsilon_1 = \epsilon_2 = 1.0$. The values of α are (a) $\alpha = 0.4318$, (b) $\alpha = 0.6364$, (c) $\alpha = 0.7800$, (d) $\alpha = 1.2614$, and (e) $\alpha = 1.3409$.

the Witney theorem states that any attractor with a maximum fractal dimension of $\nu = 1.5$ can be embedded in this $\mathbb{R}^4$ space. All the observed chaotic attractors have their measured (Grassberger-Procaccia) fractal dimension ν very close to the maximum value mentioned, which is perhaps not trivial. The number of different asymptotic dynamics that coexist in this system is surprising (at least for the authors). If we add this to the fact that only a limited number of initial conditions and parameter combinations have been explored, we get the feeling of how complex and rich the dynamics of this (apparently) simple system can be.

C. The case $\alpha\beta = 1$

As stated in Sec. II, in the case $\alpha\beta = 1$ the manifold of equilibrium points is a line in $\mathbb{R}^4$. In this case, on the other hand, the system (4) is invariant under arbitrary translations along the line of equilibrium points $z = -\alpha x$ or $x = -\beta z, y = v = 0$. In other words, if $\mathbf{r}(t)$ is a solution of (4), then

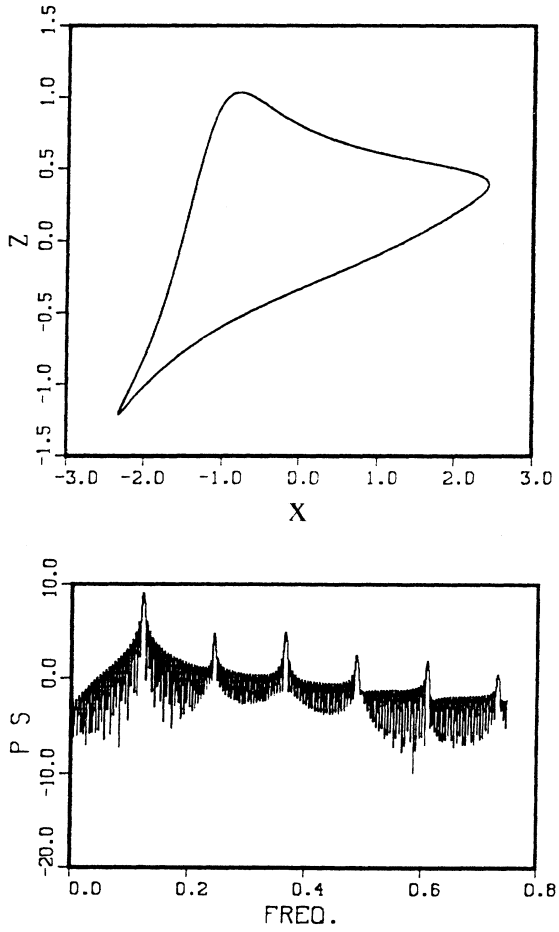

FIG. 8. Power spectrum (PS) of $x(t)$ and projection of the attractor on the plane x-z for parameter values $\epsilon_1 = \epsilon_2 = 1.0, \beta = -0.5, \alpha = 1.00$.

$$\mathbf{r}' = \begin{pmatrix} 0 & 1 & 0 & 0 \\ -1 & \epsilon_1 & -\beta & 0 \\ 0 & 0 & 0 & 1 \\ -\alpha & 0 & -1 & \epsilon_2 \end{pmatrix} \mathbf{r}_0 + \mathbf{r} \tag{18}$$

is also a solution, $\mathbf{r}_0$ being an arbitrary constant vector.

The implication of this fact is that provided we find numerically the existence of one asymptotic closed orbit, we have proven the existence of infinitely many densely packed orbits along the line of critical points. In Fig. 15 the dynamics is computed for four different initial conditions in the case where $\epsilon_1 = 1.0, \epsilon_2 = 1.0, \alpha = \beta = 1.0$, and it is shown how four different asymptotic closed orbits are obtained.

The combined theoretical plus numerical evidence proves that the case $\alpha\beta = 1$ is singular in many respects, producing a nonstandard asymptotic dynamics with infinitely many attracting closed orbits, one differing from the other in the so-called constant level over which the oscillation proceeds.

IV. CONCLUSIONS

We would like to stress the fact that the mathematical model studied here describes a very concrete physical system: a system of two van der Pol type electronic oscillators coupled by feeding one of them with a voltage proportional to the output voltage of the other and vice versa. A very interesting formal analogy between the van der Pol equation (1) and the evolution equation for the electric field of a radiation mode in a laser [14] also exists. Nevertheless, we believe that the model of two coupled electronic oscillators is the most suitable for discussing and interpreting the numerical results. Thus it may be said that the cycle is complete: The primary motivation for this work was to understand what might happen when two self-sustained oscillators are coupled in a simple way, so that a physical motivation is the basis for an abstract study on a system of evolution equations and thereafter the results obtained are reinterpreted as predictions on the physical system.

In this paper a concrete, highly symmetric coupling of two van der Pol oscillators is considered. For some combinations of coupling parameters ($\alpha\beta = 1$), a continuum

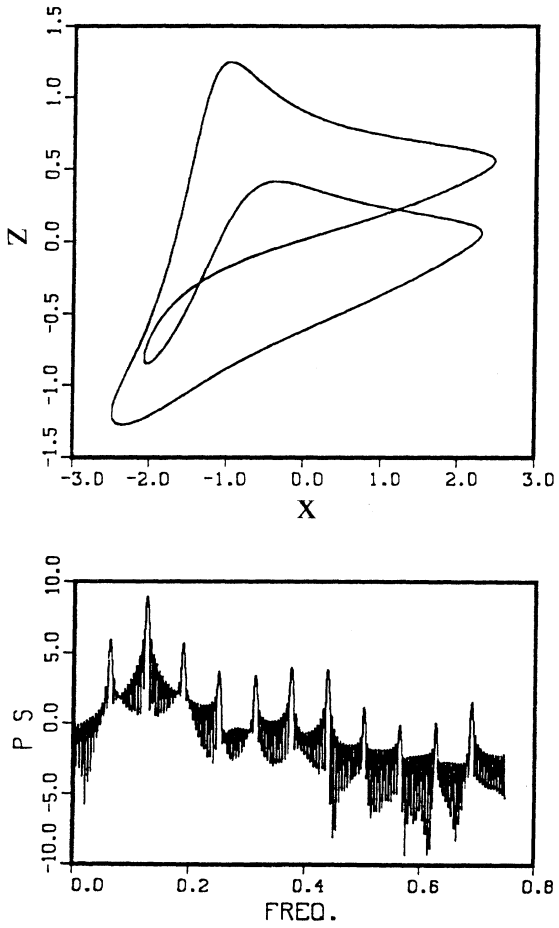

FIG. 9. Power spectrum (PS) of $x(t)$ and projection of the attractor on the plane x-z for parameter values $\epsilon_1 = \epsilon_2 = 1.0, \beta = -0.5, \alpha = 1.4$.

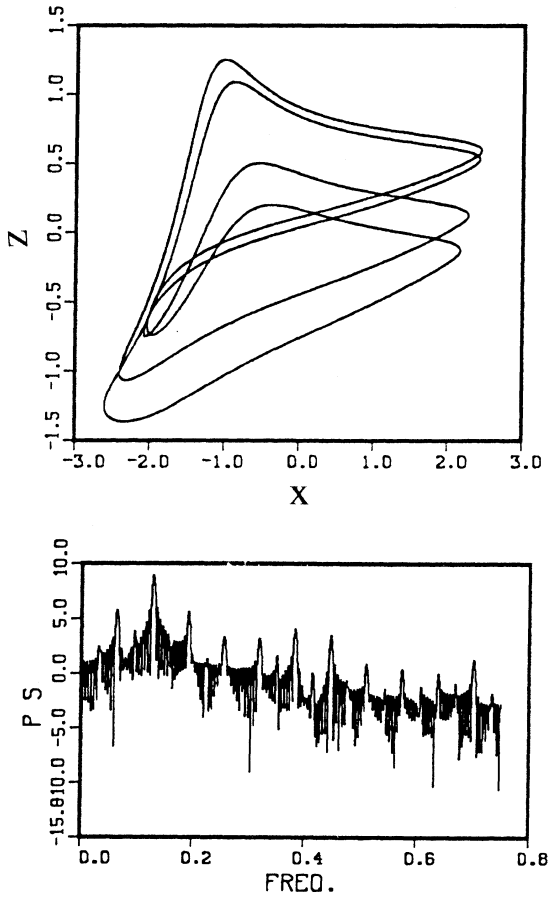

FIG. 10. Power spectrum (PS) for $x(t)$ and projection of the attractor on the plane x-z for parameter values $\epsilon_1 = \epsilon_2 = 1.0, \beta = -0.5, \alpha = 1.55$.

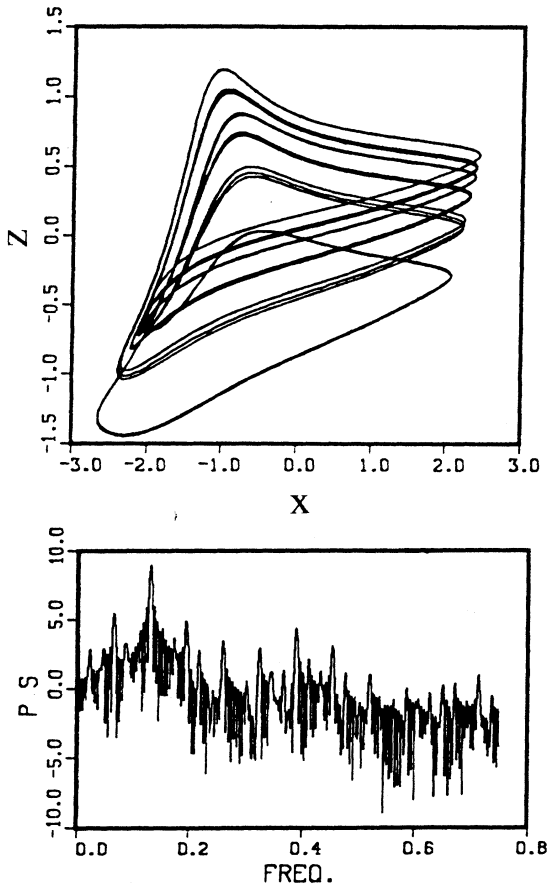

FIG. 11. Power spectrum (PS) for $x(t)$ and projection of the attractor on the plane x-z for parameter values $\epsilon_1 = \epsilon_2 = 1.0, \beta = -0.5, \alpha = 1.6$.

of equilibrium points is obtained. The combined use of a mathematical proposition and numerical evidence proves the existence of infinitely many periodic orbits, all of the same period and amplitude, but differing in the constant level over which the oscillation proceeds.

Technically speaking, we should not say that we have infinitely many limit cycles, because by limit cycle, *isolated* orbit is usually understood. Nevertheless, we believe that the result is interesting in itself, pointing to a nonstandard feature of the model equations (3).

An interesting point is that, in all cases studied, a periodic behavior in the phase space was found when the coupling parameters were both positive or negative (we are now focusing our attention on the bounded solutions). The physical meaning of this fact is that the coupling with $\alpha\beta > 0$ will induce synchronous oscillations with a common frequency, even if the uncoupled oscillators have rather different natural frequencies. This kind of behavior is commonly known as "frequency locking" and appears in many other systems of coupled nonlinear oscillators (see, for example, [18, 19]. However, a complete explanation of this widely observed fact is not yet available.

The surfaces computed in Figs. 4(a)–4(c) are then of practical interest because they allow us to know what the oscillation period and amplitudes of the coupled electronic oscillators will be as a function of the coupling parameters. Additionally, these surfaces are not trivial, in the sense that there is no general analytical way of obtaining them. This is specially true if $\alpha, \beta \simeq 1$, because for the weakly coupled system ($\alpha, \beta \ll 1$) perturbation theory could be used to obtain general results. The oscillation period diminishes as we leave the point $\alpha = \beta = 0$ along the line $\alpha = \beta$ and grows along $\alpha = -\beta$. If the

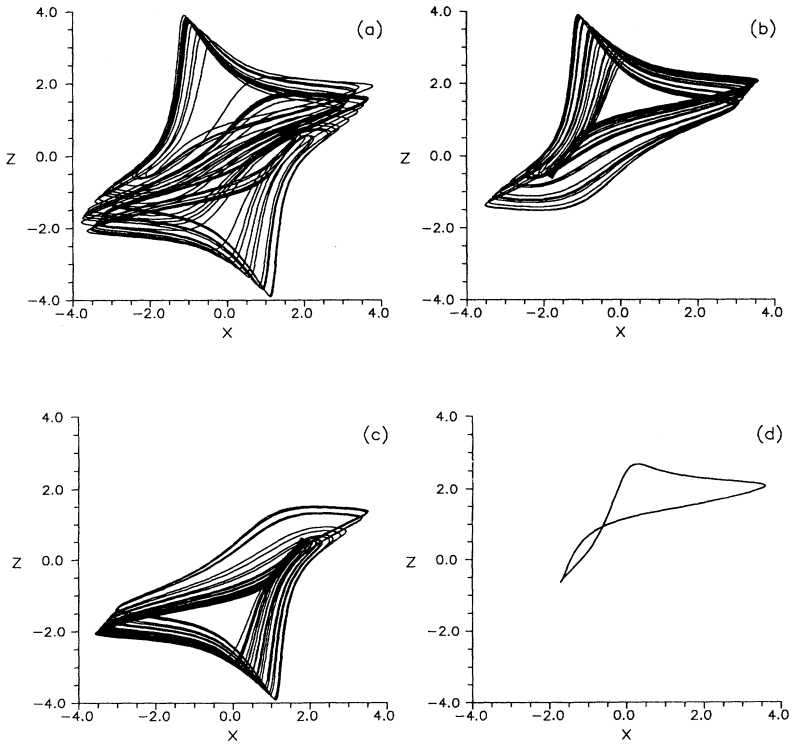

FIG. 12. Dynamics for parameter values $\epsilon_1 = 1.0, \epsilon_2 = 2.0, \beta = -0.75$. (a) The inversion symmetric strange attractor that exists for $\alpha = 0.970$. (b) and (c) The two strange attractors in which the inversion symmetric attractor splits near $\alpha = 0.9805$. (d) The limit cycle that coexists with the splitted attractors for $\alpha = 1.000$.

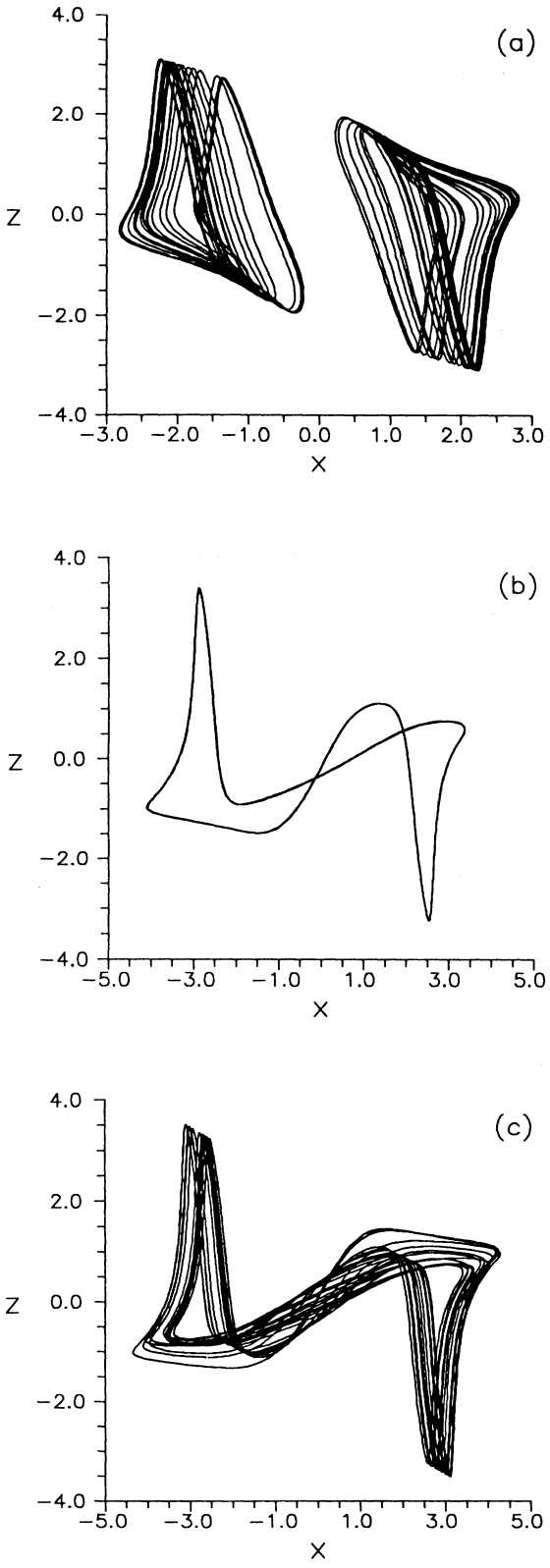

FIG. 13. Dynamics for parameter values $\epsilon_1 = \epsilon_2 = 1.0, \beta = -1.75$. (a) The two strange attractors that coexist for $\alpha = 0.480$. (b) One of the limit cycles that appears at $\alpha = 0.485$. (c) The strange attractor that arises at 0.487 coexisting with those of (a).

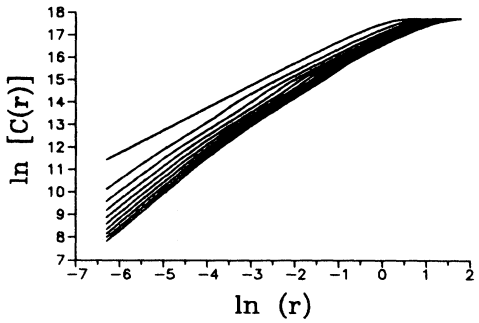

FIG. 14. Application of the GP algorithm to the symmetric attractor for $\alpha = 0.5, \beta = -1.75, \epsilon_1 = \epsilon_2 = 1.0$. The embedding dimensions vary from 1 on the upper curve to 10 on the lower one.

oscillators are different ($\epsilon_1 \neq \epsilon_2$), the oscillation amplitudes of the oscillators are generally different and are also strongly dependent on the coupling constants α and β.

The richest dynamics have been found when $\alpha\beta < 0$, and it has been observed that the more nonlinear the unperturbed oscillator is, the less the space on the $\alpha\beta$ plane is occupied by regular solutions. Then, and for some α, β values, it is possible to observe a sequence of bifurcations leading to progressively more complicated periodic oscillations and eventually to aperiodic (chaotic) ones. The above remarks could be phrased into more intuitive (or physical) terms as follows: If two van der Pol oscillators are coupled without changing the sign of any of the coupling signals (or changing *both* signs), why is synchronization is observed, while if $\alpha\beta < 0$, aperiodic oscillations take place? We do not know the answer to this question, but we think this is a problem that deserves further attention.

Symmetry considerations have been found to be relevant for the understanding and testing of our model. We have found rich dynamics in attractors creation, de-

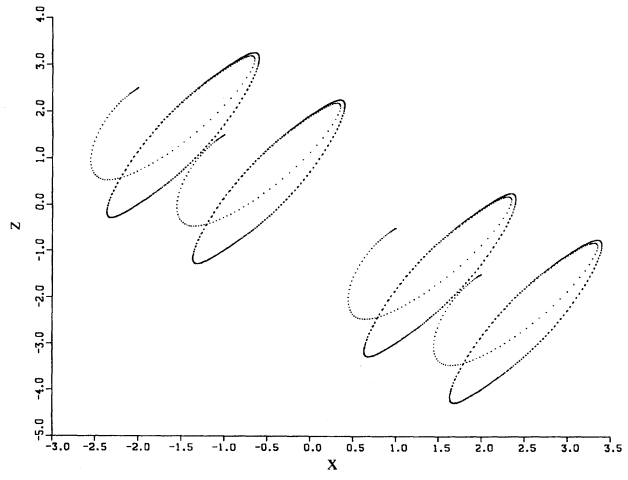

FIG. 15. Closed orbits found for four different initial conditions with $\epsilon_1 = 1.0, \epsilon_2 = 1.0, \alpha = \beta = 1.0$.

struction, splitting, and coexistence, with an interesting result showing how regular and chaotic attractors can be found together for fixed values of control parameters. The multiplicity of attractors gives rise to the possibility of hysteresis, that is, the possibility of jumping through the coexisting attractors in a way that is not reversible when we set a parameter back to its original value.

The possibility of spontaneous symmetry-breaking bifurcations has been illustrated in a very direct manner, and we would like to stress the interest of these results when, in a particular experiment, the underlying equations are not explicitly known, but some symmetries are apparent.

The calculated fractal dimension ν, which arises from the application of the Grassberger-Procaccia algorithm to the attractors observed, is such that $2\nu+1 \simeq$ (number of equations) $= 4$.

The presence of several coexisting attractors (limit cycles, chaotic attractors, or both kind of attractors simultaneously) found for some values of $\epsilon_1, \epsilon_2, \alpha, \beta$ is a fact of experimental interest, as we will try to clarify in the following. The physical system modeled by Eqs. (3) can show very different asymptotic behaviors (different mean values of the variables, clearly different averaged Fourier spectra, etc.) even if every effort is made to keep the control parameters constant. If the experimentalist is not able to select the initial conditions with exquisite precision he or she will not be generally able to predict which of the available long-term behaviors allowed will actually be selected. This fact is closely related to the very complicated structure of attracting basins. An investigation of this aspect of the problem is in course, and we can present some preliminary results showing the highly convoluted and seemingly fractal structure of the different attraction basins (Fig. 16).

The coexistence of several attractors makes it possible to end up in a different dynamics when changing a control parameter in a cyclic way (hysteresis). A nontechnical comment about this possibility in a general case can be found in [17]. In systems with many coexisting attractors, it may happen that the most practical description of the long-term behavior is a weighted average of all the possible asymptotic dynamics corresponding to the above mentioned attractors. This can be so because, sometimes, even a small quantity of random noise (unavoidable in practice) can make the system jump from one attracting basin to another. Here the weighting factors should be roughly proportional to the ratio of the measure of the different attracting basins to the total measure of the phase space that the system is allowed to explore.

FIG. 16. Structure of a section of the basins of attraction with $y = v = 0$ and x, y in $[-50, 50]$. The three tones represent the following: grey the inversion symmetric attractor, and black and white the asymmetric attractors centered on the positive and negative values of x and z, respectively. The parameter values are $\epsilon_1 = \epsilon_2 = 1.0, \beta = -1.75, \alpha = 0.487$.

For all of the above given reasons we think that the study and characterization of chaotic systems with several attractors for given control parameters values can pose key challenging experimental problems, and in such cases the use of all the symmetries associated with the system will be of utility.

Although Eqs. (3) are apparently quite simple, a great variety of behaviors has been observed, and some points are still not clear, deserving further investigation. Among them we can cite, for example, the study of the way in which attractors are created or destroyed, split or merged, the computation of two-dimensional bifurcation diagrams, and the basins of attraction for the different attractors coexisting in phase space. We plan to pursue these investigations in the near future.

ACKNOWLEDGMENTS

We want to acknowledge L. Abellanas (Departamento de Física Teórica II, Universidad Complutense) for discussions. V.M.P.-G. wants to acknowledge support from the Universidad Complutense.

* Electronic address: w281@emducm11.bitnet

[1] R.W. Boyd, M.G. Raymer, and L.M. Narducci, *Optical Instabilities* (Cambridge University Press, Cambridge, 1985).
[2] H. Haken, *Light* (North-Holland, Amsterdam, 1985), Vol. 2.
[3] G.S. Bhat, R. Narasimha, and S. Wiggins, Phys. Fluids A **2**, 1983 (1980).
[4] H.L. Swinney, Physica **7D**, 3 (1990).
[5] D. Bikany and H. Haifen, Phys. Fluids **28**, 1172 (1985).
[6] S. Quan, Y.C. Yu, and H. Chen, Phys. Fluids B **1**, 87 (1981).
[7] C. Boden and F. Mitsche, in *Nonlinear Dynamics and Quantum Phenomena in Optical Systems*, edited by R. Villaseca and R. Corbalán, Springer Proceedings in Physics Vol. 55 (Springer-Verlag, Heidelberg, 1992).
[8] van der Pol and Van der Mark, Nature **120**, 363 (1927).
[9] C. Scheffczyk, U. Parlitz, T. Kurz, W. Knop, and W. Lauterborn, Phys. Rev. A **43**, 6495 (1991).
[10] V. Englisch and W. Lauterborn, Phys. Rev. A **44**, 916 (1991).
[11] E.A. Jackson, *Perspectives on Nonlinear Dynamics* (Cambridge University Press, Cambridge, 1989).
[12] R. Poliashenko, S.R. Mckay, and C.W. Smith, Phys. Rev.

A **44**, 3452 (1991).
[13] R. Poliashenko and S.R. Mckay, Phys. Rev. A **46**, 5271 (1992).
[14] H. Haken, *Laser Theory* (Springer-Verlag, Berlin, 1970).
[15] K. Shimoda, *Introduction to Laser Physics*, 2nd ed. (Springer-Verlag, Berlin, 1986).
[16] F. Simmons, *Differential Equations with Applications and Historical Notes* (McGraw-Hill, New York, 1972).
[17] D. Ruelle, *Elements of Differentiable Dynamics and Bifurcation Theory* (Academic, New York, 1988).
[18] A.T. Winfree, J. Theor. Biol. **16**, 15 (1967).
[19] P.C. Matthews, Renato E. Mirollo, and Steven H. Strogatz, Physica D **52**, 293 (1991).

FIG. 16. Structure of a section of the basins of attraction with $y = v = 0$ and x, y in $[-50, 50]$. The three tones represent the following: grey the inversion symmetric attractor, and black and white the asymmetric attractors centered on the positive and negative values of x and z, respectively. The parameter values are $\epsilon_1 = \epsilon_2 = 1.0, \beta = -1.75, \alpha = 0.487$.